NMR Spectroscopy

Deutsche Ausgabe: DOI: 10.1002/ange.201504432
Internationale Ausgabe: DOI: 10.1002/anie.201504432

Long-Range Residual Dipolar Couplings: A Tool for Determining the Configuration of Small Molecules

*Nilamoni Nath, Edward J. d'Auvergne, and Christian Griesinger**

Abstract: *Together with NOE and J coupling, one-bond residual dipolar coupling (RDC), which reports on the three-dimensional orientation of an internuclear vector in the molecular frame, plays an important role in the conformation and configuration analysis of small molecules in solution by NMR spectroscopy. When the molecule has few C–H bonds, or too many bonds are in parallel, the available RDCs may not be sufficient to obtain the alignment tensor used for structure elucidation. Long-range RDCs that connect nuclei over multiple bonds are normally not parallel to the single bonds and therefore complement one-bond RDCs. Herein we present a method for extracting the long-range RDC of a chosen proton or group of protons to all remotely connected carbon atoms, including non-protonated carbon atoms. Alignment tensors fitted directly to the total long-range couplings ($T=J+D$) enabled straightforward analysis of both the long-range and one-bond RDCs for strychnine.*

The elucidation of the relative configuration of stereocenters of natural products can be a formidable task for organic chemists. Conventionally, NMR restraints measured in isotropic solution (that is, all orientations of a molecule are equally populated), including the NOE[1] and J coupling,[2] are used to determine the constitution of compounds[3] and yield the configuration of stereocenters in rigid compounds. This approach has proven to be difficult or impossible in cases in which the molecule is flexible or the stereocenters are remote in the bonding network.[4] In such cases, the comparison of NMR spectra of synthesized and natural products can establish the configuration,[5] although this process is cumbersome, expensive, and time-consuming, and sometimes even erroneous.[6] The prediction of chemical shifts and scalar couplings through ab initio calculations, mostly on the basis of DFT, is also utilized for the analysis of medium-sized molecules.[7] A big step forward has been taken by the introduction of RDCs into the elucidation of the conformation and configuration of small molecules, and has been made possible by the availability of alignment media for several solvents. Media compatible with solvents[8] such as $CDCl_3$ or DMSO have allowed the application of RDCs for the determination of the relative configurations of locally rigid,[9,10] semiflexible,[11] and highly flexible molecules.[12–14] Additional examples of the determination of the constitution[15] or configuration[4,16] and conformation[17] of molecules by the use of one-bond C-H RDCs ($^1D_{CH}$) extracted from ω_1- or ω_2-coupled HSQC spectra have also been reported.[18]

The above-mentioned alignment media lead to an anisotropic orientational order and consequently reintroduce parameters hidden in isotropic solvents, including RDCs[19] and RCSAs.[20] The observable coupling between a proton and a ^{13}C nucleus located n bonds away is then $^nT_{CH}={}^nJ_{CH}+{}^nD_{CH}$, in which J is the scalar coupling and D the RDC. The anisotropic orientational distribution of the compound under alignment conditions is described by the alignment tensor A,[8] which contains five independent elements and therefore requires a minimum of five linearly independent RDCs. In cases in which too few $^1D_{CH}$ values can be measured or the C–H bonds are close to parallel, the five independent RDCs required for the analysis may not be present. A special situation may arise in which all diastereoisomers of a molecule with multiple stereogenic centers fit equally well to a particular set of $^1D_{CH}$ data. Long-range RDCs (LR RDCs)—$^2D_{CH}$ and $^3D_{CH}$—can solve this problem by providing additional orientations.

A spin-flip experiment in a HSQC-based pulse sequence, named SJS-HSQC,[9] was reported for the determination of long-range RDCs for protonated carbon atoms. Although the method is sensitive because of the use of proton excitation and detection, it does not enable the determination of long-range RDCs for non-protonated carbon atoms. Herein, we describe a simple proton-selective ^{13}C-detected NMR experiment that facilitates the extraction of LR RDCs, including those of non-protonated carbon atoms. Both methods exhibit doublet splitting in the indirect dimension as $^nD_{CH}$ without homonuclear coupling and provide higher accuracy in their measurement. Since the method does not enable determination of the sign of the measured T value, a new analysis tool that operates with absolute values $|^nT_{CH}|$ is required. We show both with and without the $n=1$ couplings that it is possible to isolate the correct configuration from the 18 different configurations of the natural product strychnine by using the measured $|^nT_{CH}|$ values.

As the dipolar couplings depend on r^{-3}, where r is the distance between the two nuclei, LR RDCs are one or more orders of magnitude smaller than their one-bond counterparts. Therefore, high precision is required to extract these values. The pulse sequence used, which is conceptually similar to INEPT-based 2D experiments,[21] is presented in Figure 1. In the experiment, semi-selective inversion and refocusing pulses are applied to the proton H_i, whose coupling to remote carbon atoms is to be measured. Owing to the application of a selective refocusing pulse at the center of t_1, in-phase proton

---

[*] Dr. N. Nath, Dr. E. J. d'Auvergne, Prof. C. Griesinger
Department of NMR-based Structural Biology
Max Planck Institute for Biophysical Chemistry
37077 Göttingen (Germany)
E-mail: cigr@nmr.mpibpc.mpg.de

Supporting information for this article is available on the WWW under http://dx.doi.org/10.1002/anie.201504432.

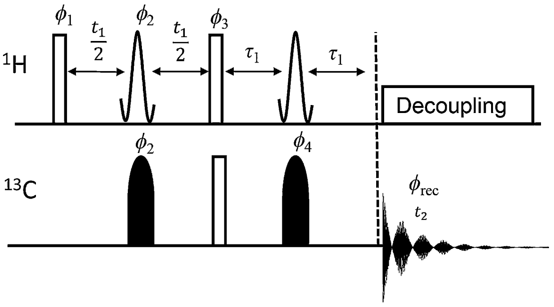

Figure 1. Pulse sequence for the proton-selective ^{13}C-detected INEPT-based experiment for the simple and systematic measurement of remote $^nJ_{CH}$ coupling constants. Narrow bars represent hard 90° pulses. The shaped ^{1}H pulses are semiselective refocusing and inversion pulses (10–25 ms at a ^{1}H frequency of 900 MHz) and Gaussian shapes applied to a proton or a group of protons whose long-range coupling constants are to be measured. All shaped ^{13}C pulses are of the adiabatic-chirp type, with durations of 2000 and 500 μs for refocusing and inversion carbon pulses, respectively. Unmarked pulses have phase x, and other pulse phases are cycled as follows: $\phi_1 = x, -x$; $\phi_2 = \phi_4 = 4(x), 4(y), 4(-x), 4(-y)$; $\phi_3 = y, y, -y, -y$; $\phi_{rec} = 2(x), 4(-x), 2(x), 2(-x), 4(x), 2(-x)$. States-TPPI (phase increment on ϕ_1) was used for the evolution time (t_1) for frequency discrimination. An RF power of 2.5 kHz for WALTZ-16 was used to decouple protons during acquisition. The τ_1 interpulse delay value was set to $(2\,^nJ_{CH})^{-1}$, where $^nJ_{CH}$ is a long-range coupling constant. The $^nJ_{CH}$ values used for isotropic and anisotropic measurement were 12 and 16 Hz, respectively.

magnetization after the first proton 90° pulse evolves only under long-range heteronuclear coupling $^nT_{CH_i}$. Following t_1 evolution, the interpulse delay ($\tau_1 = {}^nT_{CH_i}/2$) is optimized for the long-range coupling, and the selected proton H$_i$ is inverted. Refocusing of the chemical shifts during t_1 results in a simple 2D spectrum with cross-peaks split by the heteronuclear coupling in the indirect dimension. If a single proton is selectively excited, the result is a doublet for its long-range coupled ^{13}C nuclei centered at ω_1 with their respective chemical shifts in ω_2. The absolute value of the coupling without its sign, $|^nT_{CH_i}|$, is measured as the line splitting in the indirect dimension. Since the proton magnetization is transmitted through $|^nT_{CH_i}|$ to the carbon nuclei, the method enables the measurement of long-range coupling to quaternary and non-protonated carbon atoms.

Although the proton resonance of H$_i$ needs to be selectively inverted, a significant advantage is that several protons can be inverted simultaneously, provided that they do not share a common ^{13}C coupling partner. Multiplexing in this way makes it possible to reduce the number of experiments required. Usually the constitution of a molecule is known before the conformation and configuration are determined. The appropriate selection of protons to be multiplexed is not critical, as it will be obvious from non-doublets in ω_1 in the spectrum if multiplexing has been performed for the wrong protons. Spectra obtained from the inversion of several protons with a single multi-frequency-band pulse are shown in Figure 3.

Regarding sensitivity, these experiments were conducted at 900 MHz with a cryoprobe. Importantly, the measured signal-to-noise ratios in our experiment are approximately 0.8 times lower than in the SJS-HSQC experiment, yet the precision of both techniques is equal, as the experimental errors in the measured coupling values are the same (see Table S1 as well as a thorough discussion of the signal-to-noise ratio (S/N) and a comparison with proton-detected SJS-HSQC in the Supporting Information). Owing to ^{13}C detection, the performance of the method at lower magnetic fields is not significantly affected by decreased spectral resolution and sensitivity. Experimental errors in the measurement of RDCs are calculated as the standard deviation of 10 separately measured peak positions from the noise-added signals.

To demonstrate the potential of NMR spectroscopy enhanced by LR RDCs in combination with one-bond RDCs, we chose the rigid molecule strychnine (Figure 2a), which is only influenced by a single alignment tensor. The molecule was aligned in a compressed PMMA/CDCl$_3$ gel.[22] RDCs were calculated as the difference in C–H splitting under isotropic and anisotropic conditions. $^1D_{CH}$ values were measured from ^{1}H,^{13}C-CLIP-HSQC spectra.[18b] Long-range $^nD_{CH}$ values were measured by the selective inversion of protons H15a, H14, H16, H22, H15b, H8, H4, H20a, H18a, and H18b in the pulse sequence in Figure 1. The determination of the relative configuration of the adjacent stereogenic carbon-atom pairs C8/C13, C13/C14, and C12/C13 from J coupling analysis is discussed in the Supporting Information. The configurations used in the analysis were optimized by DFT at the B3LYP/6-311g(2d,p) level by using Gaussian 09[23] with the ICF-PCM solvent continuum model and CHCl$_3$ as the solvent.[24] The configurations were labeled on the basis of the R or S configuration of carbon atoms C5, C7, C8, C9, C16, and C23, in that order, for example, *SRRSRS*.

The long-range $^nJ_{CH_i}$ values ($n > 1$) can either be positive or negative. If only the absolute value of $^nJ_{CH_i}$ is known, from the measured $^nT_{CH_i}$ values, four possible LR RDC values for each bond vector can exist. $^3J_{CH}$ coupling constants are normally positive.[9] The $^2J_{CH}$ values in aliphatic systems are often negative. The $^2J_{C_{23}H_{22}}$ coupling constant present in the terminal olefinic moiety is positive as is expected for such moieties.[25] For the configurational analysis of the 18 diastereoisomers, a new technique for handling signless coupling constants was designed: The measured absolute and signless $^nT_{CH_i}$ values together with the $^nJ_{CH_i}$ values, including their predetermined signs, are used to fit an alignment tensor through nonlinear least-squares optimization. During optimization, the alignment tensor parameters θ are varied, and the resultant tensor is used to calculate signed back-calculated $^nD(\theta)$ values, which are added to the signed $^nJ_{CH_i}$ values to obtain signed $^nT(\theta)$ values. For comparison with the absolute $^nT_{CH_i}$ values, the chi-squared (χ^2) equation used in the alignment tensor optimization is constructed as:

$$\chi^2 = \sum_{i=1}^{N} \frac{\left({}^nT_{CH_i} - |{}^nT_{CH_i}(\theta)|\right)^2}{\sigma_{{}^nT_{CH_i}}{}^2} \quad (1)$$

in which N is the total number of couplings and σ is the experimental error. For the equivalent one-bond RDC equation, the $^nT_{CH_i}$ values are replaced with ^1D values, and the absolute value is removed. For the final analysis, the two χ^2 values were simply summed.

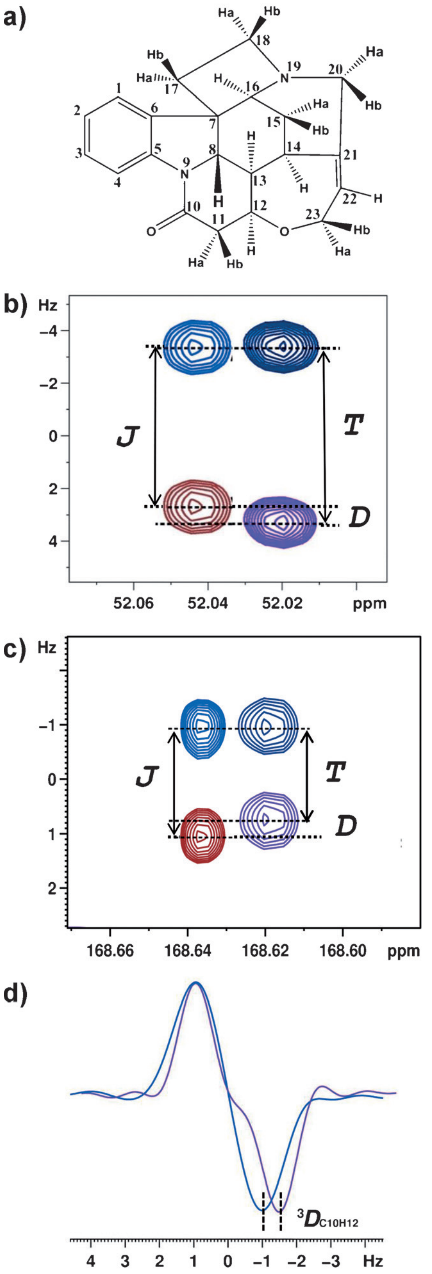

Figure 2. a) Molecular structure of strychnine with atomic numbering. b) RDC extraction: Side-by-side comparison of the H22/C20 cross-peak of the isotropic (left) and anisotropic spectra (right) when H22 was selectively refocused during t_1 and inverted during τ_1. The change in splitting of the anisotropic doublet components upon alignment as compared to the isotropic components is caused by the proton–carbon RDC. c) Side-by-side comparison of the H12/C10 cross-peak when H12 was selectively refocused and inverted during the experiment; the anisotropic splitting is smaller than the isotropic splitting. d) Superimposed plots of ω_1 slices through the H12/C10 cross-peaks of the isotropic (purple) and anisotropic (blue) spectra.

After tensor optimization, the structures were validated on the basis of quality factors (Q factors) calculated from the sum of squared errors (SSE) in the $^nT_{\mathrm{CH}_i}$ values, as normalized by the sum of squared $^nT_{\mathrm{CH}_i}$ values. This calculation corresponds to the standard definition of RDC Q factors, with $^1D_{\mathrm{CH}}$ replaced with absolute $^nT_{\mathrm{CH}_i}$. The full analysis was implemented in the software relax.[26] Optimization of the alignment tensor on the basis of only long-range coupling constants has multiple minima, but the global minimum is found readily by a grid search. As the global minimum is found in all 18 configurations, the comparison of Q values was possible and yielded the results shown in Figure 4.

Since each experiment with inversion of a selected proton provides three to five couplings, inversions of several protons resulted in a sufficient number of independent couplings. As an example, the cross-peak for the C20/H22 spin pair obtained by the selective refocusing and inversion of H22 is presented in Figure 2b. Another cross-peak that arose from the selective inversion of H12 and yielded a coupling to the non-protonated carbonyl group (C10) is shown in Figure 2c. The S/N values in the spectra are reasonable; they vary between 25 and 45 for different sets of peaks. The multiplexing 2D spectrum for which H22 and H12 were inverted together (Figure 3) enabled the extraction of several multiple-bond C–H coupling constants. Some of the cross-peaks are shown above the 2D plot for better clarity, and the overlay of cross-peaks in isotropic and anisotropic phases are shown side by side.

To investigate the impact of the LR RDCs on the analysis of the RDC data, we considered three scenarios:analysis with only $^1D_{\mathrm{CH}}$ values, analysis with only $^nT_{\mathrm{CH}}$ values, and analysis with both RDC types combined. In the case of strychnine, more than five independent one-bond RDCs are available. These RDCs enable discrimination between all 18 viable diastereoisomers. The 4 pairs of a total of 10 diastereotopic protons were assigned by the use of $^1D_{\mathrm{CH}}$ values on the basis of the Q factors (see the Supporting Information). The correct diastereomer *SRRSRS* was found to have the lowest Q factor of 0.086 (Figure 4; red bar). The next best structure is *SSRSRS* with a Q factor of 0.189. The possibility of using LR RDCs alone was explored by the construction of correlation plots of the back-calculated versus experimental absolute T values for the 18 diastereomers from only long-range couplings (see Figure S3 in the Supporting Information). As in the one-bond RDC analysis, *SRRSRS* had the lowest Q factor of 0.17 (Figure 4; yellow). The Q factor computed for the LR RDCs is slightly higher than that for the one-bond RDCs since the former are associated with a larger measurement error than the latter. The next best configuration *SSRSRS* has a sufficiently higher Q factor of 0.223, thus enabling the correct diastereomer to be isolated from long-range couplings alone. The diastereoisomers *RRRSRS* and *SSRSRS* have very similar one-bond RDC Q factors of 0.195 and 0.189, respectively. However, the Q factors for LR RDCs clearly discriminate between the two (0.543 and 0.209 for *RRRSRS* and *SSRSRS*, respectively). When analyzing a combination of one-bond and LR RDCs, we found the lowest Q factor of 0.09 for *SRRSRS* (Figure 4; blue). The next best structure is *SSRSRS* with 0.186. In the case of strychnine, any one of these three sets of coupling contants—single-bond RDCs, long-range RDCs, or their combination—can be employed for structural discrimination of the diastereomers.

To ascertain the adequacy of the LR RDC analysis, we determined the quality of the data by cross-validation of the one-bond and LR RDCs. An alignment tensor was calculated

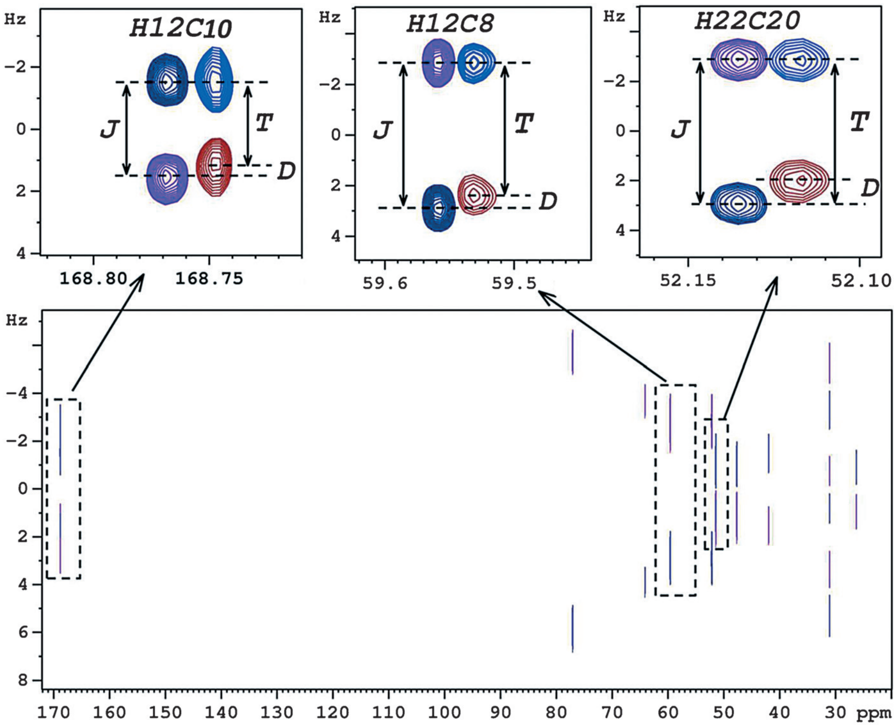

Figure 3. Multiplexed 2D spectra obtained when protons H12 and H22 were simultaneously and selectively inverted to extract several long-range CH coupling constants.

by using the one-bond RDCs and was used in turn to back-calculate LR RDCs. The experimental and back-calculated LR RDCs are in good agreement. Similarly, use of the alignment tensor calculated from the LR RDCs to back-calculate the one-bond RDCs also demonstrated the quality of the data (see the Supporting Information for the cross-validation plots).

The method for determining the alignment tensor by direct optimization against absolute $^{n}T_{\mathrm{CH}}$ values is general and can be applied to all LR RDC experiment types. It can be used for the analysis of data from the SJS-HSQC experiment,[9] but also for any new experiments which may be developed in the future. The technique removes the requirement for relative sign determination by E.COSY-type methods.[27]

The use of accurate LR RDCs extracted from the method described herein can complement the more conventional *J* coupling constants, NOEs, and one-bond RDCs. The sensitivity of the method is high as a result of the narrow line width in the detection period because of decoupling as well as homo- and heteronuclear decoupling in the indirect dimension. We used a quantity of 12 mg of strychnine in a 5 mm tube and a 5 mm cryoprobe; however, it is expected that 6 mg would suffice under anisotropic conditions. This amount could be further reduced to 1.2 mg if a 1.7 mm cryoprobe was used owing to its 5 times larger S/N for equal amounts.

It has been demonstrated that LR RDCs alone can discriminate between different configurations of strychnine in the absence of one-bond RDCs. However, the utilization of different combinations of RDCs is beneficial, as the number of experimental parameters increases, whereas the number of parameters to be fitted stays constant at five. As LR RDCs provide information complementary to that obtained from one-bond RDCs for the determination of conformation and configuration, they can be used in all situations in which one-bond RDCs are used, such as for flexible molecules, and in new cases in which one-bond RDCs are insufficient, such as for molecules with an insufficient number of independent CH vectors.

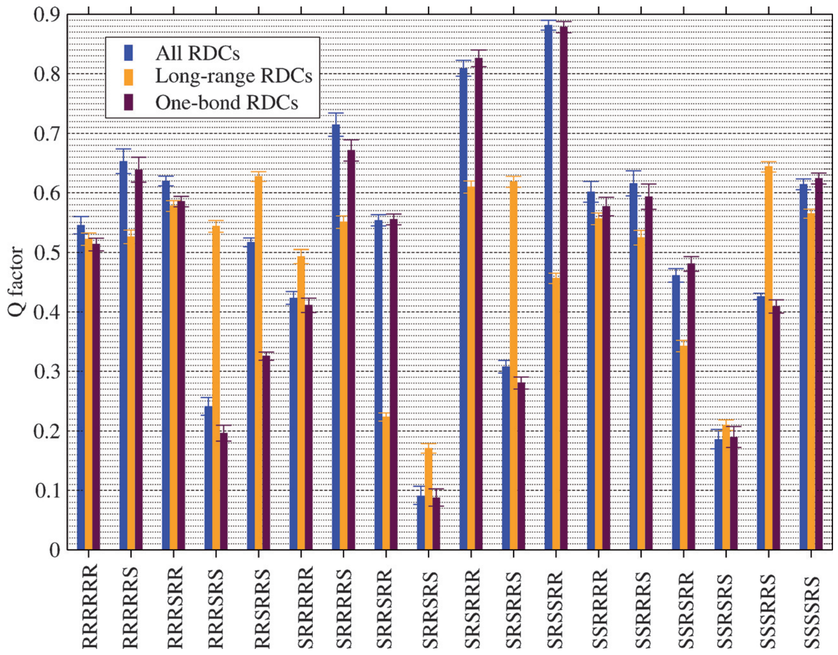

Figure 4. Strychnine RDC analysis. Comparison of quality factors (*Q*) obtained from the analysis of experimental RDC data for each viable diastereoisomer of strychnine (the lower the value of *Q*, the better the fit). Red bars: use of only one-bond coupling constants; yellow bars: use of only long-range coupling constants; blue bars: use of a combination of one-bond and long-range coupling constants.

Acknowledgements

C.G. thanks the Max Planck Society and the DFG (Forschergruppe FOR 934). We are grateful to Prof. Roberto R. Gil for providing the PMMA gel.

Keywords: configuration determination · conformation analysis · long-range residual dipolar coupling · molecular alignment · NMR spectroscopy

How to cite: *Angew. Chem. Int. Ed.* **2015**, *54*, 12706–12710
Angew. Chem. **2015**, *127*, 12897–12901

---

[1] F. A. L. Anet, A. J. R. Bourn, *J. Am. Chem. Soc.* **1965**, *87*, 5250–5251.

[2] C. A. G. Haasnoot, F. A. A. M. Deleeuw, C. Altona, *Tetrahedron* **1980**, *36*, 2783–2792.

[3] D. Neuhaus, *The Nuclear Overhauser Effect in Structural and Conformational Analysis*, 2nd ed., Wiley-VCH, New York, **2000**.

[4] H. Sun, U. M. Reinscheid, E. L. Whitson, E. J. d'Auvergne, C. M. Ireland, A. Navarro-Vázquez, C. Griesinger, *J. Am. Chem. Soc.* **2011**, *133*, 14629–14636.

[5] K. C. Nicolaou, S. A. Snyder, *Angew. Chem. Int. Ed.* **2005**, *44*, 1012–1044; *Angew. Chem.* **2005**, *117*, 1036–1069.

[6] G. Pattenden, N. J. Ashweek, C. A. G. Baker-Glenn, G. M. Walker, J. G. K. Yee, *Angew. Chem. Int. Ed.* **2007**, *46*, 4359–4363; *Angew. Chem.* **2007**, *119*, 4437–4441.

[7] a) M. G. Chini, R. Riccio, G. Bifulco, *Magn. Reson. Chem.* **2008**, *46*, 962–968; b) G. Bifulco, P. Dambruoso, L. Gomez-Paloma, R. Riccio, *Chem. Rev.* **2007**, *107*, 3744–3779.

[8] a) P. Haberz, J. Farjon, C. Griesinger, *Angew. Chem. Int. Ed.* **2005**, *44*, 427–429; *Angew. Chem.* **2005**, *117*, 431–433; b) L. Arnold, A. Marx, C. M. Thiele, M. Reggelin, *Chem. Eur. J.* **2010**, *16*, 10342–10346; c) N. C. Meyer, A. Krupp, V. Schmidts, C. M. Thiele, M. Reggelin, *Angew. Chem. Int. Ed.* **2012**, *51*, 8334–8338; *Angew. Chem.* **2012**, *124*, 8459–8463; d) C. Merle, G. Kummerlöwe, J. C. Freudenberger, F. Halbach, W. Stower, C. L. von Gostomski, J. Hopfner, T. Beskers, M. Wilhelm, B. Luy, *Angew. Chem. Int. Ed.* **2013**, *52*, 10309–10312; *Angew. Chem.* **2013**, *125*, 10499–10502; e) G. Kummerlöwe, J. Auernheimer, A. Lendlein, B. Luy, *J. Am. Chem. Soc.* **2007**, *129*, 6080–6081; f) J. C. Freudenberger, P. Spiteller, R. Bauer, H. Kessler, B. Luy, *J. Am. Chem. Soc.* **2004**, *126*, 14690–14691; g) G. Kummerlöwe, E. F. McCord, S. F. Cheatham, S. Niss, R. W. Schnell, B. Luy, *Chem. Eur. J.* **2010**, *16*, 7087–7089.

[9] P. Trigo-Mouriño, A. Navarro-Vázquez, J. F. Ying, R. R. Gil, A. Bax, *Angew. Chem. Int. Ed.* **2011**, *50*, 7576–7580; *Angew. Chem.* **2011**, *123*, 7718–7722.

[10] P. Trigo-Mourino, R. Sifuentes, A. Navarro-Vazquez, C. Gayathri, H. Maruenda, R. R. Gil, *Nat. Prod. Commun.* **2012**, *7*, 735–738.

[11] A. Schuetz, J. Junker, A. Leonov, O. F. Lange, T. F. Molinski, C. Griesinger, *J. Am. Chem. Soc.* **2007**, *129*, 15114–15115.

[12] A. Schuetz, T. Murakami, N. Takada, J. Junker, M. Hashimoto, C. Griesinger, *Angew. Chem. Int. Ed.* **2008**, *47*, 2032–2034; *Angew. Chem.* **2008**, *120*, 2062–2064.

[13] C. Farès, J. Hassfeld, D. Menche, T. Carlomagno, *Angew. Chem. Int. Ed.* **2008**, *47*, 3722–3726; *Angew. Chem.* **2008**, *120*, 3782–3786.

[14] a) C. M. Thiele, A. Marx, R. Berger, J. Fischer, M. Biel, A. Giannis, *Angew. Chem. Int. Ed.* **2006**, *45*, 4455–4460; *Angew. Chem.* **2006**, *118*, 4566–4571; b) C. M. Thiele, *Eur. J. Org. Chem.* **2008**, 5673–5685; c) C. M. Thiele, A. Maliniak, B. Stevensson, *J. Am. Chem. Soc.* **2009**, *131*, 12878–12879.

[15] G. Kummerlöwe, B. Crone, M. Kretschmer, S. F. Kirsch, B. Luy, *Angew. Chem. Int. Ed.* **2011**, *50*, 2643–2645; *Angew. Chem.* **2011**, *123*, 2693–2696.

[16] a) M. E. García, S. Pagola, A. Navarro-Vázquez, D. D. Phillips, C. Gayathri, H. Krakauer, P. W. Stephens, V. E. Nicotra, R. R. Gil, *Angew. Chem. Int. Ed.* **2009**, *48*, 5670–5674; *Angew. Chem.* **2009**, *121*, 5780–5784; b) R. R. Gil, C. Gayathri, N. V. Tsarevsky, K. Matyjaszewski, *J. Org. Chem.* **2008**, *73*, 840–848.

[17] M. B. Schmid, M. Fleischmann, V. D'Elia, O. Reiser, W. Gronwald, R. M. Gschwind, *ChemBioChem* **2009**, *10*, 440–444.

[18] a) G. Kummerlöwe, B. Luy, *TrAC Trends Anal. Chem.* **2009**, *28*, 483–493; b) A. Enthart, J. C. Freudenberger, J. Furrer, H. Kessler, B. Luy, *J. Magn. Reson.* **2008**, *192*, 314–322.

[19] N. Tjandra, A. Bax, *Science* **1997**, *278*, 1697–1697.

[20] F. Hallwass, M. Schmidt, H. Sun, A. Mazur, G. Kummerlöwe, B. Luy, A. Navarro-Vázquez, C. Griesinger, U. M. Reinscheid, *Angew. Chem. Int. Ed.* **2011**, *50*, 9487–9490; *Angew. Chem.* **2011**, *123*, 9659–9662.

[21] a) K. Y. Ding, *J. Magn. Reson.* **1999**, *140*, 495–498; b) A. Bax, *J. Magn. Reson.* **1984**, *57*, 314–318.

[22] a) C. Gayathri, N. V. Tsarevsky, R. R. Gil, *Chem. Eur. J.* **2010**, *16*, 3622–3626; PMMA = poly(methyl methacrylate); b) J. D. Snider, E. Troche-Pesqueira, S. R. Woodruff, C. Gayathri, N. V. Tsarevsky, R. R. Gil, *Magn. Reson. Chem.* **2012**, *50*, S86–S91.

[23] Gaussian 09, Revision C.01, M. J. Frisch, G. W. Trucks, H. B. Schlegel, G. E. Scuseria, M. A. Robb, J. R. Cheeseman, G. Scalmani, V. Barone, B. Mennucci, G. A. Petersson, H. Nakatsuji, M. Caricato, X. Li, H. P. Hratchian, A. F. Izmaylov, J. Bloino, G. Zheng, J. L. Sonnenberg, M. Hada, M. Ehara, K. Toyota, R. Fukuda, J. Hasegawa, M. Ishida, T. Nakajima, Y. Honda, O. Kitao, H. Nakai, T. Vreven, J. A. Montgomery, Jr., J. E. Peralta, F. Ogliaro, M. Bearpark, J. J. Heyd, E. Brothers, K. N. Kudin, V. N. Staroverov, T. Keith, R. Kobayashi, J. Normand, K. Raghavachari, A. Rendell, J. C. Burant, S. S. Iyengar, J. Tomasi, M. Cossi, N. Rega, J. M. Millam, M. Klene, J. E. Knox, J. B. Cross, V. Bakken, C. Adamo, J. Jaramillo, R. Gomperts, R. E. Stratmann, O. Yazyev, A. J. Austin, R. Cammi, C. Pomelli, J. W. Ochterski, R. L. Martin, K. Morokuma, V. G. Zakrzewski, G. A. Voth, P. Salvador, J. J. Dannenberg, S. Dapprich, A. D. Daniels, O. Farkas, J. B. Foresman, J. V. Ortiz, J. Cioslowski, D. J. Fox, Gaussian, Inc., Wallingford CT **2010**.

[24] B. Mennucci, J. Tomasi, *J. Chem. Phys.* **1997**, *106*, 5151–5158.

[25] J. L. Marshall, *Methods in Stereochemical Analysis*, *Vol. 2*, Wiley-VCH, Weinheim, **1983**.

[26] E. J. d'Auvergne, P. R. Gooley, *J. Biomol. NMR* **2008**, *40*, 107–133.

[27] H. Schwalbe, P. Schmidt, C. Griesinger, *Coupling Constants Determined by ECOSY in Encyclopedia of Magnetic Resonance*, Wiley, Hoboken, **2007**.

Received: May 15, 2015
Revised: July 14, 2015